CHAPTER SIX

TRICK: A Single-Molecule Method for Imaging the First Round of Translation in Living Cells and Animals

J.M. Halstead[*,1], J.H. Wilbertz[*,†,1], F. Wippich[†], T. Lionnet[§], A. Ephrussi[‡], J.A. Chao[*,2]

[*]Friedrich Miescher Institute for Biomedical Research, Basel, Switzerland
[†]University of Basel, Basel, Switzerland
[‡]European Molecular Biology Laboratory, Heidelberg, Germany
[§]Transcription Imaging Consortium, HHMI Janelia Research Campus, Ashburn, VA, United States
[2]Corresponding author: e-mail address: jeffrey.chao@fmi.ch

Contents

[1] These authors contributed equally to this work.

Methods in Enzymology, Volume 572
ISSN 0076-6879
http://dx.doi.org/10.1016/bs.mie.2016.02.027

Abstract

The life of an mRNA is dynamic within a cell. The development of quantitative fluorescent microscopy techniques to image single molecules of RNA has allowed many aspects of the mRNA lifecycle to be directly observed in living cells. Recent advances in live-cell multicolor RNA imaging, however, have now made it possible to investigate RNA metabolism in greater detail. In this chapter, we present an overview of the design and implementation of the translating RNA imaging by coat protein knockoff RNA biosensor, which allows untranslated mRNAs to be distinguished from ones that have undergone a round of translation. The methods required for establishing this system in mammalian cell lines and *Drosophila melanogaster* oocytes are described here, but the principles may be applied to any experimental system.

1. INTRODUCTION

Messenger RNA (mRNA) translation is tightly regulated to produce protein at the correct time and place with appropriate abundance. While many of the principles of translation regulation have been elucidated from ensemble biochemical measurements, understanding the mechanisms controlling where and when an mRNA is translated within a single cell is an emerging research goal. Indeed, considerable evidence now suggests that regulation of translation is devolved to specific cytoplasmic compartments, and that well-timed mRNA translation at a defined location is critical to several physiological processes, ranging from synaptic plasticity (Holt & Schuman, 2013), axis specification (Kumano, 2012), and cell motility (Liao, Mingle, Van De Water, & Liu, 2015). Understanding the mechanistic basis of localized translation regulation therefore requires spatial and temporal information to be extracted from single translation events in single living cells.

While technical advances have expanded the toolbox available to measure translation, spatial and temporal information are rarely simultaneously acquired. Ribosome profiling maps transcriptome-wide ribosome occupancy to subcodon resolution, providing a powerful readout of translation

on the timescale of minutes (Ingolia, Ghaemmaghami, Newman, & Weissman, 2009). Spatial information, however, is either restricted to particular organelles (Jan, Williams, & Weissman, 2014) or lost altogether. Imaging assays for translation provide broad spatial information by labeling components of the translational machinery (Pan, Kirillov, & Cooperman, 2007), or the nascent polypeptide itself (David et al., 2012; Dieterich et al., 2010; Terskikh et al., 2000). While these approaches have elegantly demonstrated that protein production is locally regulated within subcellular domains, they do not measure single translation events in real time. Recently, the fluorescence of single protein molecules has been used to detect local translation events; however, maturation of fluorescent proteins (FPs) occurs several minutes after translation (Ifrim, Williams, & Bassell, 2015; Tatavarty et al., 2012; Yu, Xiao, Ren, Lao, & Xie, 2006).

To detect single translation events with high temporal and spatial resolution in living cells, we developed an RNA biosensor that enables identification of untranslated mRNAs from ones that have undergone at least one round of translation (Halstead et al., 2015). This technique relies on the ribosome removing a unique fluorescent signal from the coding sequence of a transcript during the first round of translation. We refer to this methodology as translating RNA imaging by coat protein knockoff (TRICK).

In this chapter, we describe the steps to design, express, acquire, and analyze data from the TRICK system. Particular attention is given to expressing TRICK transgenes at levels appropriate for single-molecule RNA imaging and to acquiring and analyzing two-color imaging data. Though emphasis is given to establishing the TRICK system in mammalian cell lines and *Drosophila melanogaster*, many of the principles described here are applicable to other experimental systems.

2. DESIGN OF TRICK REPORTER mRNAs

Considering translation from the perspective of a transcript has the advantage that robust methods have been developed that allow detection of single molecules of mRNA in living cells using fluorescent microscopy. The highly specific interaction between the MS2 bacteriophage coat protein (MCP) and its cognate RNA stem-loop has been extensively used to image RNAs in many experimental systems ranging from bacteria to mouse neurons (Urbanek, Galka-Marciniak, Olejniczak, & Krzyzosiak, 2014). This strategy relies on insertion of multiple copies of the MS2 stem-loop (usually 24) within the 3′-untranslated region (UTR) of a transcript of interest and

the binding of a chimeric fusion of MCP with a FP to these sequences. Since the transcripts are bound by many fluorescent MCP-FPs, the mRNAs appear as bright diffraction-limited spots that can be detected above the background of the unbound MCP-FP. The inclusion of a nuclear localization sequence (NLS) to MCP-FP increases imaging sensitivity, because the unbound NLS-MCP-FP is concentrated in the nucleus, which enables rapid labeling of MS2 transcripts during transcription and reduces background in the cytoplasm (Fusco et al., 2003).

In order to take advantage of the spectrum of FPs that have been created, a number of other RNA–protein complexes have been engineered to visualize mRNAs (Chen et al., 2009; Daigle & Ellenberg, 2007; Takizawa & Vale, 2000). Given the success of the MS2 system, we developed the PP7 bacteriophage coat protein (PCP) that binds to a unique RNA stem-loop as an orthogonal RNA-labeling system (Chao, Patskovsky, Almo, & Singer, 2008; Larson, Zenklusen, Wu, Chao, & Singer, 2011). Using the MS2 and PP7 systems together allows simultaneous single-molecule RNA imaging of two distinct species of transcripts within a living cell and also enables the possibility of labeling a single mRNA within two different regions of the transcript (Coulon et al., 2014; Hocine, Raymond, Zenklusen, Chao, & Singer, 2013; Martin, Rino, Carvalho, Kirchhausen, & Carmo-Fonseca, 2013).

The act of translation requires that a ribosome traverses the coding sequence of an mRNA thereby decoding the information contained within a transcript in order to synthesize polypeptides. Consequently, any RNA-binding proteins that are bound to the transcript within the coding sequence must be removed by the ribosome. In particular, the exon junction complex, a multiprotein complex deposited upstream of exon–exon boundaries during splicing, is displaced by the ribosome during the first round of translation and therefore identifies transcripts that have never been translated (Ishigaki, Li, Serin, & Maquat, 2001). We reasoned that it should be possible to engineer a fluorescent RNA biosensor based upon this principle that would enable untranslated mRNAs to be distinguished from ones that had undergone at least one round of translation.

In order to construct an RNA biosensor to image the first round of translation, we designed PP7 stem-loops that could be translated by the ribosome that permitted the labeling of a transcript within the coding sequence (PP7) and the 3′-UTR (MS2) (Fig. 1A). When this transcript is untranslated, it will be bound by the two coat proteins fused to distinct FPs (eg, NLS-PCP-GFP and NLS-MCP-RFP) and will appear yellow when imaged because it will be labeled by both green and red FPs (Fig. 1B). During the first round of

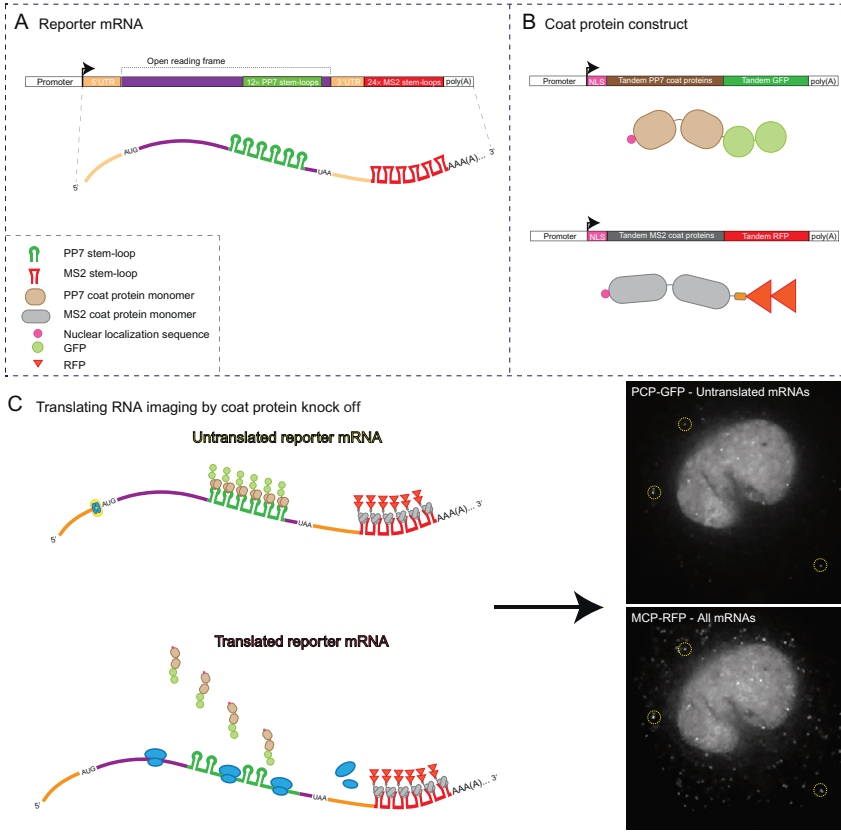

Fig. 1 Translating RNA imaging by coat protein knockoff. (A) TRICK reporter transcript contains translatable PP7 stem-loops in the open reading frame and MS2 stem-loops in the 3′-UTR. (B) PP7 and MS2 bacteriophage coat proteins are fused to spectrally distinct fluorescent proteins (eg, NLS-PCP-GFP and NLS-MCP-RFP). The addition of nuclear localization sequences (NLS) results in accumulation of unbound fluorescent proteins in the nucleus. (C) Untranslated mRNAs are bound by both fluorescent fusion proteins while translated mRNAs are labeled with only NLS-MCP-RFP. Dual-color RNA imaging can distinguish single molecules of untranslated mRNAs that are fluorescent in both *green* and *red channels* (*yellow circles*) from those that have been translated and are detected in the *red channel* alone.

translation, however, the ribosome will strip the NLS-PCP-GFP signal from the transcript resulting in the appearance of a red mRNA that is labeled with only NLS-MCP-RFP. Since the concentration of NLS-PCP-GFP is low in the cytoplasm, rebinding of NLS-PCP-GFP is not favorable and the displaced FP returns to the nucleus (Fig. 1C).

Since it is possible to design translatable RNA sequences for any of the RNA–protein complexes used to image RNAs, we have outlined the principles we used to design the PP7 stem-loops. The first MS2 stem-loops used to image RNAs were constructed by PCR by making two copies of the stem-loops that could then be multimerized by ligation with DNA fragments digested using restriction enzymes that generate compatible cohesive ends (eg, *Bam*HI and *Bgl*II) (Bertrand et al., 1998). Consequently, adjacent MS2 stem-loops were spaced by 20 nucleotides due to limitations, at the time, on the synthesis of large DNA oligonucleotides. A translating ribosome, however, produces a footprint of ~30 nts on a transcript, and we found that tight spacing of stem-loops results in a significant block of translation (Ingolia et al., 2009; Steitz, 1969). By spacing PP7 stem-loops farther apart (40 nts), we found that the ribosome could efficiently translate through them. Since the PP7 stem-loops will encode a polypeptide, we removed stop codons from the open reading frame and optimized codon usage for expression in mammalian cells by considering both codon frequency and coding potential. RNA folding was assessed using the *mfold* software to confirm that all PP7 stem-loops were predicted to fold correctly (Zuker, 2003).

Initially, a cassette containing six copies of the PP7 stem-loops was synthesized and tested for its translatability when fused to the C-terminus of a reporter gene. While western blot analysis revealed that the PP7 stem-loops were efficiently translated, imaging of this construct was difficult due to the low signal-to-noise ratio resulting from the small number of stem-loops. A 12×PP7 cassette was then generated which improved imaging of single mRNA molecules without inducing adverse effects on translation. In instances when addition of the polypeptide encoded by the PP7 stem-loops is not desirable (eg, labeling of endogenous genes), the addition of self-cleaving 2A sequences between the C-terminus of the protein of interest and the stem-loops may be advantageous (Kim et al., 2011). We have also found that it is possible to place the PP7 stem-loops within the N-terminus of a reporter gene, which may facilitate experiments designed to measure translation initiation rates by reducing the effect of ribosome elongation.

3. TRICK EXPERIMENT IN MAMMALIAN CELLS

3.1 Expression of TRICK Reporter Transcripts

The TRICK system provides a fluorescent readout from three transgenes, a reporter mRNA and two coat proteins, each of which must be expressed at appropriate levels in the same cell. Selecting the appropriate promoter to drive expression of the reporter mRNA is therefore key to designing a

TRICK experiment. As the TRICK system reports on the first round of translation only, there are advantages to controlling precisely when the reporter mRNA is expressed. While constitutive expression produces a mixed population of reporter transcripts that have been transcribed at different time points, including those transcribed and translated before imaging began, an inducible promoter can provide a population of nascent mRNAs whose pioneer round of translation is restricted to the experimental window. As a result, inducible expression of reporter mRNA is better suited to many experiments, particularly those examining the temporal regulation of translation. We found that both the tetracycline- and ponasterone A-inducible systems are well suited for performing TRICK experiments (Gossen et al., 1995; No, Yao, & Evans, 1996).

TRICK reporter mRNAs can be expressed from plasmids that are transiently transfected or stably integrated into the genome. Transient transfection is relatively fast and simple, with constitutive reporter mRNA expression peaking 24–48 h after transfection by lipid-based reagents, and can allow different TRICK reporters to be rapidly tested. Delivery of DNA plasmids by transient methods, however, can result in significant cell-to-cell variation in expression levels that can complicate image analysis. As it is possible to determine the translational status of every single TRICK reporter mRNA within a cell, the most meaningful quantitative comparisons are between cells expressing similar numbers of transcripts and at levels comparable to endogenous transcripts. It is possible to transiently transfect and identify cells within a heterogeneous population that meet this criteria, however, this limits data acquisition to a relatively small number of cells per experiment. Instead, reproducible and more uniform expression is best achieved by stably integrating the TRICK reporter into the cell genome by either random or site-specific integration. We have found that site-specific integration of an inducible TRICK reporter by recombinase-mediated cassette exchange to be an efficient method for generating TRICK cell lines. In this system, reporter mRNA expression is consistent across cells thereby limiting experimental variability. We use a HeLa cell line that contains both the rtTA2-M2 tetracycline reverse transactivator required for doxycycline-inducible expression and a single RCME site that allows stable integration of TRICK reporter mRNAs (Weidenfeld et al., 2009).

3.2 Expression of Coat Proteins Fused to Fluorescent Proteins

The crux of the TRICK experiment is to spectrally distinguish translated and untranslated mRNAs. Consequently, the appropriate selection and

expression of the coat protein (CP; PCP and MCP)–FP pairs is critical to the success of the experiment. The CP-FPs used in the TRICK experiment must be fused to spectrally distinct fluorophores that are suitable for single-molecule RNA imaging. Both CP-FPs must also be expressed at cellular levels that allow robust labeling of all reporter mRNAs and, importantly for the TRICK experiment, do not favor rebinding of PCP-FP to the transcript once it has been displaced by the ribosome in the cytoplasm.

Single-molecule two-color imaging of mRNAs requires that the coat proteins are fused to fluorophores that satisfy a number of criteria. Foremost, as TRICK requires unambiguous separation of two fluorescent signals, spectrally distinct fluorophores must be selected to label each coat protein. Overlap of emission spectra and cross-excitation of overlapping absorption bands can be avoided by judicial choice of fluorophores. As a result, optimal imaging requires that distinct fluorophores are also matched to the light source and filters that will be used to acquire data.

Within these criteria, brightness, the product of quantum yield and extinction coefficient, and photostability, the decrease in emission over sequential excitation events, are the leading properties for fluorophore selection. This is particularly important for single-particle tracking (SPT) experiments because single mRNAs must be imaged multiple times and photobleaching of one channel can bias analysis. Genetically encoded FPs, such as GFP, exist in a range of spectra (Shaner, Steinbach, & Tsien, 2005) and have been successfully used in a number of single-molecule RNA imaging studies. We have found that NLS-PCP-EGFP and NLS-MCP-TagRFP-T are compatible with two-color RNA imaging with short ($\leq$50 ms) exposure times. Other FPs can be used to suit other imaging modalities, however, the properties must fit the experiment parameters. For example, while tdTomato (extinction coefficient = 138,000 M^{-1} cm^{-1}, quantum yield = 0.69) is brighter than TagRFP-T (extinction coefficient = 81,000 M^{-1} cm^{-1}, quantum yield = 0.41), tdTomato is significantly less photostable and less suitable for time-lapse imaging (Shaner et al., 2008). The recent development of alternative intracellular fluorescent labeling technologies, including the Halo-Tag, Snap-Tag, and Clip-Tag, can also be used to conjugate chimeric coat proteins to inorganic dyes (Gautier et al., 2008; Juillerat et al., 2003; Los et al., 2008). This approach allows the coat proteins to be specifically covalently bonded to inorganic dyes such as tetramethylrhodamine-based dyes, which are bright (extinction coefficient = 101,000 M^{-1} cm^{-1}, quantum yield = 0.88) and significantly more photostable than FPs (Grimm et al., 2015).

While inducible promoters are useful for controlling acute and robust reporter mRNA transcription, CP-FPs are best expressed constitutively at low levels. A number of constitutive promoters are commonly used, including SV40, CMV, UbiC, EF1a, PGK, and CAGG variants, of which PGK and UbiC have been found to reproducibly give lower expression levels (Qin et al., 2010). We have found that lentiviral transduction is an efficient means to stably express CP-FPs (Lionnet et al., 2011). Cells can be coinfected with two viruses each encoding a different CP-FP and cells that are double positive can be isolated by fluorescence-activated cell sorting (FACS). Successive rounds of FACS followed by fluorescent microscopy can be used to generate cell lines that express both CP-FPs at levels suitable for two-color single-molecule RNA imaging. The use of tandem single-chain dimers of the MS2 and PP7 coat proteins enables cells to be sorted for very low levels of the FPs without disrupting the RNA-binding function of the coat proteins (Wu, Chao, & Singer, 2012; Wu et al., 2015).

3.3 Considerations and Challenges of TRICK in Primary Cells

Balancing CP-FPs and TRICK reporter mRNA expression is particularly challenging in primary cells. Unless the cells are derived from an animal stably expressing the TRICK transgenes, both the reporter mRNA and CP-FPs must be introduced. While stable transgene integration followed by FACS of positive cells is optimal in cell lines, many primary cells can only be passaged a limited number of times and growing a sufficient number cells from a sorted population may not be possible.

In particular, primary neurons present a number of challenges for establishing single-molecule two-color RNA imaging. First, neurons are postmitotic and transient transfection rates are low. While other means of delivering transgenes (eg, infection using lentiviruses or electroporation) are more efficacious, a small percentage of cells will express the transgenes at appropriate levels that must be individually identified by fluorescence microscopy during each experiment. To increase the number of positive cells in a primary culture, the both CP-FP constructs can be expressed in a single bicistronic plasmid separated by an internal ribosome entry site (IRES), or a 2A peptide sequence. It is necessary to ensure that the CP-FPs are expressed properly because IRES-driven expression is typically lower than cap-dependent translation (Mizuguchi, Xu, Ishii-Watabe, Uchida, & Hayakawa, 2000) and 2A peptide sequences can produce chimeric fusion proteins that will undermine TRICK analysis (Kim et al., 2011).

3.4 Controls

To confirm that any TRICK construct gives a precise readout of translation, it is necessary to test if the insertion of either of the stem-loops or the binding of the CP-FPs perturbs reporter mRNA metabolism. The stability of the TRICK reporter mRNA can be assessed by real-time PCR following inhibition of transcription, either by small-molecules (eg, actinomycin D) or washing away activators of inducible promoters. The translation of the TRICK reporter construct should also be confirmed by western blotting to demonstrate that a protein of appropriate molecular weight is produced. It is also advantageous for the TRICK reporter to encode a protein with a functional readout (eg, fluorescence, bioluminescence, or enzymatic activity). We have found it useful for TRICK reporters to encode Renilla or Firefly luciferase because translation can be measured using a common luciferase assay that can be correlated with imaging data. Control experiments should be performed both with and without stem-loops and with and without coexpression of CP-FPs (Table 1). This approach will identify any element of the TRICK construct that affects reporter stability or translation and provides a starting point for troubleshooting.

4. MICROSCOPY

The success of a TRICK experiment largely depends on its accurate imaging readout. The field of live-cell single-molecule imaging has utilized different light microscopy variants, broadly characterized into epi-fluorescence wide-field, confocal, and total internal reflection fluorescence (TIRF) microscopy. Each of these microscopy setups offers certain advantages and drawbacks when dual-color single mRNAs, as in TRICK, are to be imaged in live cells.

4.1 Imaging Modality

A straightforward and cost-effective way of imaging single RNA molecules in live cells is conventional wide-field or epifluorescence microscopy. Here, a collimated/parallelized beam of light illuminates the entire thickness of the sample, resulting in a large field-of-view and a high number of molecules that can potentially be tracked. This advantage however comes at the price of a large fraction of out-of-focus light, resulting in high background levels and reduced single-molecule detection. Wide-field microscopy is therefore especially suited for specimens with a low number of fluorescent molecules

Table 1 Controls for TRICK Reporter mRNA Expression

Control Experiment	Reporter mRNA Expression	CP-FP Expression	Method
Is reporter mRNA stability affected by stem-loops?	1. TRICK reporter lacking stem-loops 2. TRICK reporter with stem-loops in the coding region and 3′-UTR	None	Measurement of mRNA half-life by real-time PCR. Northern blotting of mRNA
Is reporter mRNA stability affected by CP-FP binding?	TRICK reporter with stem-loops in the coding region and 3′-UTR	1. CP-FP bound to the coding region 2. CP-FP bound to the 3′-UTR 3. CP-FPs bound to both the coding region and 3′-UTR	Measurement of mRNA half-life by real-time PCR. Northern blotting of mRNA
Is reporter mRNA translation affected by stem-loops?	TRICK reporter with stem-loops in the coding region and 3′-UTR	None	Measurement of protein MW and levels by Western blot
Is reporter mRNA translation affected by CP-FP binding	TRICK reporter with stem-loops in the coding region and 3′-UTR	1. CP-FP bound only to the coding region 2. CP-FP bound only to the 3′-UTR 3. CP-FPs bound to both the coding region and 3′-UTR	Measurement of protein MW and levels by Western blot
Is the translated reporter protein functional?	TRICK reporter with stem-loops in the coding region and 3′-UTR	CP-FPs bound to both the coding region and 3′-UTR	Functional readout of protein activity (eg, fluorescence, bioluminescence, enzymatic activity)

and a thin imaging volume (a few microns or less), causing low background fluorescence. Consequently, cells with a small thickness such as yeast, bacterial, and epithelial cells or certain cellular extensions such as axons are well suited to be imaged by wide-field microscopy.

As opposed to wide-field microscopy, a confocal illumination scheme effectively reduces out-of-focus light and thereby enables the recording of high-contrast images in all spatial dimensions. Focusing the laser beam

to the size of a diffraction-limited spot and using a pinhole aperture that rejects all light emitted outside of the focal volume are the two key elements to the spatial filtering of out-of-focus light. However, the confocal illumination scheme suffers from two major drawbacks. Since only a single diffraction-limited spot is illuminated at a time, the focal plane needs to be scanned point-by-point by either moving the sample or the laser beam, as in traditional laser scanning confocal microscopy (LSCM). Secondly, the pinhole aperture filters out a large fraction of the total light used for sample excitation. In combination, loss of emitted light and point-by-point scanning lead to long pixel dwell times to collect enough photons and long scanning times because relevant field-of-views typically require 10^5–10^6 pixels, resulting in a low frame rate that can become limiting when imaging rapidly moving mRNA molecules. Spinning-disk confocal microscopy has been developed as a faster alternative, and we have successfully used it for TRICK experiments. In spinning-disk microscopy, a first disk with a large number of spirally oriented microlenses is rotating at high speed and essentially focuses thousands of split laser beams on the sample. A second spinning disk, with a spiral array of pinholes, is aligned to the first and blocks all out-of-focus light. As a result, the fast, synchronized disk rotation and spiral orientation of microlenses and pinholes enables the near-simultaneous scanning of a single imaging plane. While allowing the high temporal resolution (subsecond frame intervals) required for TRICK experiments, a spinning-disk confocal microscope suffers from reduced fluorescence intensity detection due to beam splitting and the use of pinholes. Rapid photobleaching due to out-of-focus fluorescence excitation is another major limitation of all confocal microscopy approaches.

Reducing photobleaching is imperative during TRICK experiments. The pair of fluorophores that fluorescently label reporter mRNAs usually have different sensitivities to photobleaching. If one fluorophore bleaches faster than the other, the detection efficiency of the corresponding fluorophore will vary over the time of one experiment and might result in a bias toward incorrect identification of translational state. One way to reduce photobleaching (as well background fluorescence due to out-of-focus excitation) is to use an optical sectioning method called TIRF microscopy. TIRF is based on the observation that a collimated laser beam propagating through one medium when reaching a second medium is reflected at the interface, if a large enough angle and appropriately different refractive indices of the two media are chosen. The reflection creates an exponentially decaying evanescent wave in the z-direction within the sample, allowing

only the excitation of molecules within a few hundred nanometers within the sample and leading to an excellent reduction of bleaching and high contrast. While TIRF can be a good option for live-cell imaging, it allows only the imaging of molecules close to the sample-glass interface, making it impossible to image and detect TRICK transcripts deep inside of the cell. Furthermore, the rapidly decreasing intensity of the evanescent wave with increasing distance from the coverslip leads to a wide distribution of fluorescent particle brightnesses—a substantial challenge for quantitative analysis. Another optical sectioning method is more widely applicable to imaging TRICK reporter mRNAs and allows for the detection of translation in all cellular compartments. Here, an inclined laser beam just below the critical angle for TIRF is used. Instead of creating an evanescent wave, the laser beam now passes directly into the sample, but in the form of a highly inclined laminated optical sheet (HILO) with a thickness in the low micrometer range (Tokunaga, Imamoto, & Sakata-Sogawa, 2008). A rotating mirror ensures that the sample is illuminated from all angles. Because any form of point scanning is not necessary, high frame rates can be achieved. We have successfully applied HILO to perform TRICK experiments in live cells. HILO offers low amounts of out-of-focus light, low bleaching, and fast image acquisition rates.

4.2 Light Source

Since a large number of fluorophores with excitation–emission spectra ranging from near-ultraviolet, visible, to near-infrared regions are currently available (Kremers, Gilbert, Cranfill, Davidson, & Piston, 2011; Xia, Li, & Fang, 2013), it is often most appropriate to match the required fluorophores to the already existing illumination setup.

Two spectrally distinct lasers constitute the illumination source of choice (especially for confocal imaging) since they provide a narrowly defined excitation wavelength range, low divergence when passing through the optical setup, and high excitation power. Gas lasers such argon or krypton ion lasers or solid-state lasers such as diode lasers are most commonly used. For dual-color imaging, the most important criterion when choosing a light source is to maximize the fluorophores excitation efficiency while minimizing excitation cross talk. For dual-color mRNA imaging with the described MS2 and PP7 system, 488 and 561-nm emitting lasers have been found to be appropriate to excite the commonly used FPs such as GFP or RFP-variants while providing sufficiently separated emission spectra. More information

on how to optimize the laser excitation of various fluorophores for live-cell imaging has been described elsewhere (Xia et al., 2013).

For wide-field microscopy, cost-effective alternatives to laser excitation can be used, eg, arc-discharge lamps such as mercury or xenon arc lamps, or more recently light-emitting diodes (LEDs) (Cho et al., 2013; Gerhardt, Mai, Lamas-Linares, & Kurtsiefer, 2011; Higashida et al., 2008). The commonly used mercury-based arc lamps typically display intensity peaks at certain wavelengths and therefore do not provide an even intensity across the full light spectrum. These considerations are important when deciding on a light source for simultaneous dual-color imaging. Xenon-based arc lamps display a more even intensity profile, but lack the shorter wavelength range typically employed for fluorescent microscopy. A third form of arc-discharge-based light sources is metal-halide lamps. This type of lamp combines the properties of xenon and mercury, resulting in an even, high intensity emission across the entire light spectrum from ultraviolet to infrared. The use of LEDs for dual-color RNA imaging is currently limited since the detection of single molecules has so far only been demonstrated in the close blue and green spectra (Gerhardt et al., 2011; Kuo, Kuyper, Allen, Fiorini, & Chiu, 2004). Recently, white LEDs have been used for super-resolution microscopy in live cells (Cho et al., 2013) and might represent an attractive alternative to laser light sources for dual-color single-molecule imaging in the future.

4.3 Signal Detection

For TRICK experiments, it is key to detect both fluorescence channels unambiguously to avoid a systematic analysis bias toward one of the channels and incorrect conclusions about the translation state. Signal bleed-through due to overlapping fluorophore emission spectra can be effectively minimized by appropriate design of the bandpass excitation and emission barrier filters and should be controlled for. mRNA particles can travel relatively fast with diffusion coefficients up to 3.42 $\mu m^2\ s^{-1}$ (Ma et al., 2013) and transport rates of $\approx 1.3\ \mu m\ s^{-1}$ (Park et al., 2014). The mRNA's image on the camera chip can therefore move by one pixel or more between frames, even when imaging at subsecond intervals. Consequently, it is crucial to image the two-color channels simultaneously in order to unambiguously identify dual-labeled particles. As a consequence, filter cube switching is not an option for TRICK imaging. Instead, the best setup for the microscope emission path is to first separate the emission light from the excitation source with

a multiline dichroic mirror, followed by a second dichroic mirror that will split the collected fluorescence in two beams (eg, GFP vs RFP fluorescence). The two beams can then be imaged by two separate cameras or recombined on the two halves of the same camera chip.

The two most used camera types include scientific complementary metal oxide semiconductor (sCMOS) and electron multiplying charge coupled device (EMCCD) cameras. Due to the coupling of photon detection and voltage conversion at the physical pixel level on the chip, sCMOS cameras allow for high-speed imaging of more than 100 frames s^{-1}. The consequence is a relatively high internally generated background (dark noise) and readout noise, limiting the photon sensitivity under low light conditions, as is the case for single-molecule RNA imaging. In contrast, EMCCD cameras achieve single-photon sensitivity. Despite having a lower chip readout speed, which is generally still permissive for single mRNA tracking, EMCCD cameras currently offer significant advantages over other types of camera sensors, especially when applied under low emitted light conditions.

TRICK experiments require the acquisition of both fluorescent channels simultaneously in order to guarantee signal colocalization. The solution of choice to image relatively large biological structures (eg, an entire mammalian cell, typically tens of microns across) is to separately collect the fluorescence from the two channels on two well-aligned cameras. At a magnification that permits the detection of single molecules, the use of two cameras provides a large enough field-of-view in each fluorescent channel to fully capture the sample. A practical alternative to the costly dual-camera approach is the use of a split chip on a single camera. Here, the image is divided into two spatially equivalent, but separate halves on the camera chip. Postimaging registration of both halves of the chip into a single image can be performed.

4.4 Temperature and CO_2 Control

Translation is very sensitive to changes in the extracellular environment. TRICK live-cell experiments therefore require strictly physiological conditions during imaging. Mammalian cells generally require an incubation temperature of 37°C and a CO_2 atmosphere of 5–7% to maintain an appropriate pH, depending on the growth medium. The humidity level should also be controlled in order to prevent excessive evaporation and drying. Several commercial systems are available to keep the biological sample under these

physiological conditions during imaging. A simple and inexpensive method is to use heating elements directly adjacent to the objective and sample dish. Repeated cycles of heating and cooling, however, lead to thermal movements of the objective and the sample itself leading to a loss of focus over time. While less economical, a Plexiglas incubation box, which fully encloses the microscope body, is more suitable for live-cell imaging. A second cover that seals with the stage can then be placed on top of the specimen to regulate CO_2 and humidity within this restricted volume.

5. DATA COLLECTION

The quantification of data obtained from TRICK experiments involves two major steps. First, all mRNA particles per imaging frame need to be detected in each of the two respective channels. Then the detected particle positions in consecutive frames are combined to give individual mRNA trajectories in a computational process termed SPT. To avoid detection biases toward one channel based on the different fluorophore properties, the acquired imaging data needs to be of high quality by fulfilling the two following major criteria: first, the signal-to-noise ratio (SNR) needs to be as high as possible, while, second, the imaging frame rate needs to be sufficiently high to connect the positions of individual mRNAs over time (Park, Buxbaum, & Singer, 2010).

5.1 Considerations for Single-Molecule Detection and Tracking

A major limitation of live-cell imaging experiments is that a high SNR and frame rate will lead to rapid photobleaching and phototoxicity caused by an excessive amount of photons hitting the specimen. Finding a balance between frame rate, exposure time, and excitation power is therefore key to being able to image and subsequently track single mRNAs in two colors (Magidson & Khodjakov, 2013).

Because of the diffraction of light, individual fluorescent particles appear as spots of a few 100 nm in size when imaged through a microscope. The shape of the spot depends on the microscope and the fluorophore and is called the point spread function (PSF). The spatial profile of the PSF on the camera is nearly Gaussian, which makes it possible through fitting to measure the position of each particle center with high accuracy (typically $\approx$40 nm). If the PSF is spread onto a large number of camera pixels, each spot becomes hard to separate from the background and readout noise. Conversely, if the spot on the image is concentrated onto a single pixel, it is hard

to achieve a high localization precision through fitting. A high SNR is therefore typically obtained by combining a high numerical aperture objective (which means a high light collection power), and a magnification optimized for single-molecule imaging. In practice, magnifications that yield 100–200 nm per pixel tend to give optimal localization precision for single-molecule tracking (Thompson, Larson, & Webb, 2002). As images of mRNA labeled in separate colors need to be registered, chromatic aberrations pose a significant challenge. They are minimized by using apochromatic objectives and can be corrected postacquisition using adequate calibration techniques, eg, using multicolor beads or fiducial markers within the sample (Grunwald & Singer, 2010).

Diffusion coefficients of mRNAs have been shown to range from 0.009 to 3.42 $\mu m^2\ s^{-1}$ depending on the type of transcript and subcellular localization (Fusco et al., 2003; Ma et al., 2013; Mor et al., 2010; Shav-Tal et al., 2004). Therefore, exposure times need to be long enough for a good SNR while being short enough to prevent blurring of fast moving mRNA particles. In addition, the frame rate needs to be short enough to reliably track an mRNA's position from frame-to-frame. Exposure times and frame rates should therefore be optimized based on each system's dynamic range, ensuring unbiased detection while minimizing oversampling and photobleaching. In cases where very fast frame rates and short exposure times are crucial, but the chip readout speed is limiting, it is possible to readout only a subarray of the chip, thereby decreasing the total required readout time per frame at the expense of a reduced field-of-view.

Besides optimizing the frame rate, other means to increase the SNR can be used, such as pixel binning. During pixel binning a group of pixels on the camera chip (eg, 2×2 pixels) are binned together and assigned to a single pixel value during the readout of the chip. A 2×2 binning for example increases the signal fourfold (four times more photons per pixel) at the cost of a twofold lower resolution (pixel information is lost). Finally, optimizing the camera gain and the chip readout speed can also improve the SNR and dynamic range. Slower chip readout speeds result in lower readout noise and can be compensated for by utilizing only a subarray of the chip, as described earlier.

5.2 Considerations for Long Time-Lapse Experiments

The TRICK technique can be used to study translation regulation with subcellular resolution over a wide range of time scales: from fast, single-molecule dynamics movies (subsecond frame rates covering a few seconds

to minutes) to longer, time-lapsed acquisitions matching the dynamics of cellular responses (minutes to hours). Minimizing photobleaching by the previously described imaging optimizations is key for successful longer time-lapse experiments. Although the detailed mechanism of photobleaching is not entirely known, photo-oxidation of the fluorophores is thought to be caused by reactive oxygen species (ROS). The addition of chemical compounds such as ascorbic acid (vitamin C) (Vigers, Coue, & McIntosh, 1988), trolox (a vitamin E derivative) (Rasnik, McKinney, & Ha, 2006), mercaptoethylamine (Widengren, Chmyrov, Eggeling, Lofdahl, & Seidel, 2007), or enzymatic deoxygenation systems (Aitken, Marshall, & Puglisi, 2008) has been shown to delay photobleaching. Since oxygen plays an important role in cell physiology, the use of ROS scavengers can have unwanted effects that need to be taken into account.

Stage stability over long time periods in all three spatial dimensions is crucial for long-term live-cell experiments. Especially when heated incubation chambers are used, it is important to thermally equilibrate the whole microscope body, including the stage, prior to the experiment in order to prevent thermal drift and to avoid permanent refocusing. Motorized Piezo stages that are equipped with reflection-based rather than image-based autofocus systems minimize manual interventions during an experiment.

Some adherent cell types growing on coverslips can move extensively in the x,y dimension even on the order of minutes and might require the use of cell motion tracking (Rabut & Ellenberg, 2004). Several software packages that can be coupled to the appropriate microscope hardware are currently available by commercial suppliers.

6. ANALYSIS

Dual-color single-molecule mRNA imaging during a TRICK experiment allows direct observation of two distinct translational states depending on the presence of one or both fluorophores. In order to reconstruct the trajectories of individual mRNA particles and determine their translation state, multiple computational steps must be performed (Fig. 2). First one needs to identify and localize discrete particles on each acquired image (Fig. 2A); this step outputs a list of particle positions for each time point and color channel (Fig. 2B). The second step consists of tracking the particles, which means connecting together the spot positions that correspond to the same particle at different times, yielding a list of trajectories for each color channel (Fig. 2C). Finally, one sorts the trajectories present in both channels

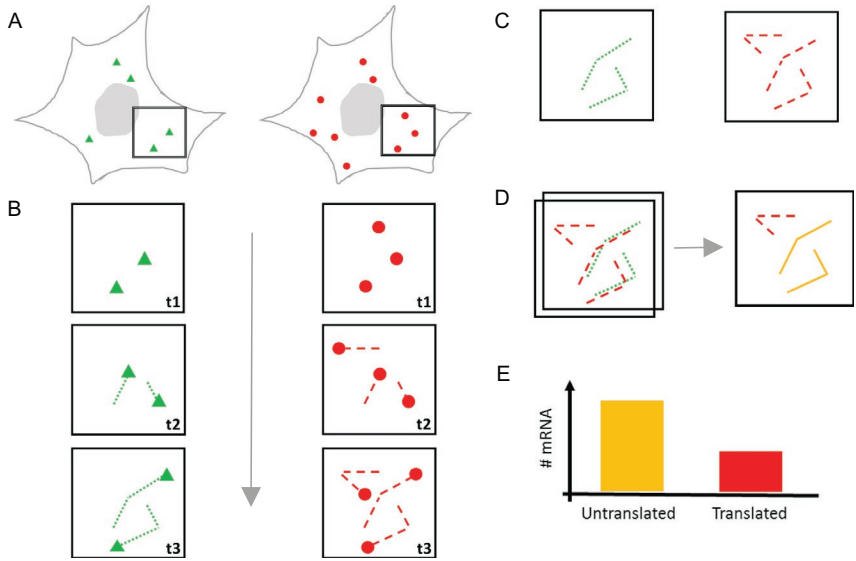

Fig. 2 Schematic depiction of the analysis workflow for a TRICK experiment in living cells. (A) Each cell is imaged simultaneously in two colors, resulting in two fluorescent channels. Here, the mRNAs labeled with NLS-PCP-GFP and NLS-MCP-RFP are depicted by *triangles* and *circles*, respectively. (B) After image acquisition all mRNA diffraction-limited spots in each imaging frame are detected. Spot detection is best performed individually for each fluorescent channel. (C) Next, spot tracking is performed. Here, the spot positions in each frame are taken into account and tracks for each mRNA molecule are calculated. (D) The resulting tracks from both fluorescent channels originating from the same cell are then assessed for colocalization. *Red* (*dark gray* in the print version) and *green* (*light gray* in the print version) mRNA tracks represent the same dual-colored molecule when a significant overlap exists. (E) mRNAs that have been determined to be dual-colored are considered to be untranslated, while single *red* (*dark gray* in the print version) colored mRNAs have been translated at least once.

(corresponding to dual-labeled untranslated mRNA) from those present in a single channel only (single-labeled translated mRNAs) (Fig. 2D and E). Measuring the spatiotemporal evolution of single- vs dual-color-labeled molecules then gives an indication about the localization and translational status of the mRNAs.

6.1 Single-Molecule Detection and Tracking

Detection and tracking of single particles should be performed for each fluorescent channel individually (Fig. 2A and B). A number of commercially and freely available software packages exist that combine detection and tracking

of all single particles in each frame within a given image sequence in two consecutive steps in a semiautomated manner. Different particle tracking approaches have recently been extensively tested and reviewed by Chenouard et al. (2014). In general particle detection and tracking should be performed on unprocessed data that have been recorded according to the earlier described principles in order to maximize the SNR and to fulfill the Nyquist criterion on temporal sampling so that individual particles can be tracked over time (Park et al., 2010). The precise particle detection and tracking methodology needs to be chosen based on the data quality, particle density, and intended tracking time frame. For the detection of single particles several approaches exist. Maxima-based detection relies on the identification of the highest local pixel values, which are then defined as spots. Thresholding utilizes the principle of a particle's higher intensity over the surrounding background based on an appropriate intensity threshold. More accurate (and computationally intensive) approaches involve PSF fitting and centroid estimation. Fitting often relies on the PSF-based fitting of a Gaussian intensity distribution to each spot candidate or uses other linear or nonlinear models. Centroid estimation detects diffraction-limited spots by determination of the radial spot center, which often does not coincide with the local maximum and is a reliable method to distinguish neighboring spots (Parthasarathy, 2012).

Once spots have been detected and their positions evaluated, one needs to connect the spots in order to generate trajectories (Fig. 2C). The simplest method to achieve this connects each spot with its nearest neighbor in the next frame, allowing for only a limited displacement range (based on knowledge of the typical transport properties of the biological species), and a given number of gaps—false negatives are common in single-molecule tracking because fluorescence of a particle might be intermittently obscured by noise or background, resulting in a missed detection. Multiframe or multitrack and motion model-based tracking approaches are more sophisticated techniques that go beyond frame-to-frame nearest-neighbor linking and are suitable for live-cell mRNA imaging. They are robust against partial detection failures and crossing trajectories. Multiframe or multitrack approaches take the history of a tracked particle into account in order to match it to a future estimated trajectory. Motion-based models fit the trajectories to typical single-particle movement patterns such as Brownian motion, corralled diffusion, or directed motion (Park et al., 2010). The most robust particle tracking methods rely on a combination of several of the aforementioned detection and tracking approaches (Chenouard et al., 2014). Because it is technically difficult using wide-field epifluorescence or confocal microscopy

to acquire 3D volumes at frame rates compatible with single-molecule tracking with sufficient SNR, single mRNA tracking has mostly been performed in 2D planes where particle movement in and out-of-focus limits the observation time to a few seconds in ideal cases. However, innovative microscopy approaches have recently been developed to overcome this issue and collect 3D trajectories of mRNA particles (Smith et al., 2015; Spille et al., 2015). These imaging modalities circumvent the problem of particles moving out-of-focus and are able to generate longer trajectories; the tracking analysis techniques are conceptually identical to those used for 2D tracking.

Although long trajectories are ideal to investigate the fate of individual mRNA molecules, short observations times are not necessarily limiting to determine the translation state of a two-color-labeled mRNAs (Fig. 2). Short trajectories of a few 100 ms are often sufficient to reliably determine the degree of colocalization of an mRNA population within a cell.

6.2 Determining Colocalization of Tracked Two-Colored mRNA Particles

The determination of colocalization between both fluorescent channels is key to determine translation, as in the case of TRICK or other dynamic properties probed by a two-color mRNA imaging experiment. Since every field-of-view typically contains a large number of tracked mRNAs, colocalization between the two trajectory data sets is best performed in an automated fashion (Deschout et al., 2013; Dupont, Stirnnagel, Lindemann, & Lamb, 2013; Koyama-Honda et al., 2005).

One important first step in colocalization is to ensure one can accurately register the two-color channels. This calibration is usually performed by imaging small ($\approx$100 nm) fluorescent beads or gold nanorods that emit a broad spectrum of light spanning the two channels used in the experiment. Each bead produces one diffraction-limited spot in each channel. By using detection algorithms to measure the position of each bead image in the separate channels, one can calculate the spatial transformation needed to precisely map the position of the red beads onto the green ones. This process corrects for systematic chromatic aberrations (specific to one microscope because of the properties of its lenses, but invariant over time) and misalignments. As microscopes can substantially drift over time, it is important to perform these calibration routines frequently, ideally on a daily basis if one desires to achieve high registration accuracies. Typical registration errors can be as small as 5–10 nm. The spatial transformation generated during the calibration is then applied to the measured spots after the experiment, before matching them to the second channel.

Algorithms carrying out this kind of colocalization have been described in more detail before (Espenel et al., 2008; Halstead et al., 2015). Although in principle one could assess colocalization at each time point by matching positions of green and red spots, this strategy is very sensitive to missed or spurious detections, which are not uncommon when tracking individual molecules in the low SNR regime. We found that a more effective approach consists of matching trajectories rather than individual spot positions (Fig. 2D). The reason is that tracking algorithms are designed to accommodate both false negatives (short gaps are usually allowed in trajectories) and false positives (only trajectories longer than a few frames are considered, which cleans up spurious detections). As a result, matching trajectories rather than spots is a robust way to assess colocalization at the single-molecule level.

The algorithm to match trajectories consists of measuring the spatiotemporal overlap between all green and red trajectories. If two trajectories are found to be within a certain distance threshold of one another (typical value in our experiments is 100 nm) for a certain number of frames (typical value in our experiments is three frames), then they are scored as colocalized. Even though the number of frames used as our colocalization criterion might seem small, longer colocalized trajectories are usually visibly moving together for their entire duration. Perfect trajectory overlap is often not achievable, because of the uncertainty in measuring the position of each spot (in our conditions, around 40 nm in x,y), and the error in registering the two channels together ($\approx$15 nm). This algorithm works best when the particles are bright and well separated in space, but is robust in a wide range of SNR and concentrations typical of single-molecule tracking. One advantage of TRICK is that out of three potential trajectory combinations (red only, green only, and colocalized red + green), one only expects to observe two: red only (3′-UTR label only for translated mRNAs) and colocalized green + red (both ORF and 3′-UTR label for untranslated mRNAs) because the 3′-UTR red label always remains bound to its target. Therefore, the measurement carries an internal control: the number of colocalized trajectories over the total number of green trajectories (green only and colocalized) is a direct metric of the experimental sensitivity (typical values in our experiments 80–90%). The results can be expressed as colocalization percentages per cell (Fig. 2E), indicating for example the amount of translated mRNA at different time points after reporter induction. Trajectories can then be analyzed separately to investigate the relative importance of location, transport, and dynamic properties of various mRNA translation states.

6.3 Controls

It is important to bracket imaging experiments with positive and negative controls. Imaging and performing particle detection on cells lacking CF-FPs should not reveal fluorescent signal. Similarly, imaging cells expressing CF-FPs, but not the reporter mRNA, should show diffuse CP-FP signal in the nucleus only, and no bright single particles. To determine if every mRNA is detectable via live-cell imaging, TRICK can be combined with single-molecule fluorescence in situ hybridization (mRNA FISH). In fixed cells, multiple singly labeled fluorescent FISH probes robustly detect single reporter mRNAs, which should correspond to the same number of mRNAs detected in live cells by CP-FPs. Imaging the entire cell volume in a 3D stack can confirm that every reporter mRNA is fluorescently labeled by coat proteins.

Under steady state conditions in mammalian cells $\approx$6% of our standard reporter mRNAs are untranslated and so fluoresce in both red and green channels, while $\approx$94% of mRNAs are translated and appear in the red channel only. Imaging cells expressing only one CP-FP in both channels should yield no colocalization and controls for fluorophore cross talk. As a positive control for detection of colocalization, both stem-loop cassettes can be inserted into the reporter 3′-UTR, which should result in 100% of mRNAs that fluoresce in both channels independent of translation. This is a particularly useful control for optimizing the colocalization of two-color trajectories from SPT data.

Inhibitors of translation can demonstrate that the TRICK signal (loss of fluorescence from the coding sequence) is translation-dependent and serve as a powerful control. Small-molecule inhibitors affecting different steps of translation can be used as complementary controls (eg, puromycin causes premature termination and cycloheximide halts elongation).

7. TRICK EXPERIMENT IN HeLa CELLS TO DETERMINE FRACTION OF UNTRANSLATED mRNAs

7.1 Preparation of Cells for Live-Cell Imaging

Materials

- Tetracycline-inducible HeLa cells stably expressing NLS-PCP-GFP, NLS-MCP-Halo, and a TRICK reporter mRNA containing PP7 (coding region) and MS2 (noncoding region) stem-loops

- Dulbecco's Modified Eagle Medium (DMEM; Life Technologies, 10566-016) supplemented with 10% (v/v) Tet-free FBS (Clontech, 631106) and 1% (v/v) penicillin and streptomycin (pen/strep)
- 35 mm μ-Dish (Ibidi, 81158)
- Automated cell counter and counting slides (Biorad, D9891-1G)
- Doxycycline (Sigma, D9891-1G)
- JF_{549} (HHMI Janelia Research Campus)

Day 1

1. HeLa cells are grown using standard cell culture techniques as adherent monolayers in DMEM + 10% FBS + 1% Pen/Strep.
2. Prepare a cell suspension of HeLa cells at a density of 20,000 cells mL^{-1} and ensure dissociation into single cells.
3. Seed 2 mL of cell solution per 35 mm imaging dish. Care should be taken in order to obtain a homogenous distribution of cells within the dish.
4. Incubate 2 days at 37°C and 5% CO_2. Shorter incubation periods are also possible depending on the time it takes for cells to attach and spread on the surface of the imaging dish.

Day 3

1. Prewarm PBS and DMEM + 10% FBS to 37°C.
2. Halo-label cells by addition of 1 mL 100 n*M* JF_{549} in DMEM + 10% FBS.
3. Return cells to incubator (37°C, 5% CO_2) for 15 min.
4. Remove medium and wash cells 3 × with PBS.
5. Replace medium with 37°C warm DMEM + 10% FBS containing 1 $\mu g\ mL^{-1}$ doxycycline to induce TRICK reporter expression.

7.2 Image Acquisition

Materials

- Olympus IX81 inverted microscope (Olympus) equipped with a Yokogawa CSU-X1 scanhead (Yokogawa) and Borealis modification (Andor)
- Dichroic beam-splitter in scanhead (Semrock Di01-T488/568-13x15x0.5)
- 100 × 1.45NA PlanApo TIRFM oil immersion objective (Olympus)
- Two back-illuminated EvolveDelta EMCCD cameras (Photometrics)
- Emission filters for GFP (Semrock, FF01-617/73-25) and JF_{549} (Semrock, FF02-525/40-25) fluorescence

- Beam-splitter between cameras (Chroma, 565DCXR)
- Solid-state lasers (100 mW 491 nm and 100 mW 561 nm; Cobolt)
- Motorized X,Y,Z-Piezo controlled stage (ASI)
- Incubation box around microscope providing heating and CO_2 regulation (Life Imaging Services)

Day 3

1. Equilibrate microscope imaging chamber to 37°C and 5% CO_2.
2. Select cells for imaging using MCP-Halo channel by identifying cells that contain well-resolved diffraction-limited particles (spot width ~2 pixels). Image using low laser power to limit photobleaching before acquisition of TRICK data.
3. Simultaneously image cells in both channels using laser powers, camera gain, and exposure times compatible for SPT. Exposure times should be 40–50 ms or less, in order to ensure that fast moving mRNPs can still be unambiguously tracked between subsequent frames. Laser power optimization is a tradeoff: high laser powers result in bright, well-resolved particles that are easier to track, but induce rapid photobleaching. Once adequate exposure and laser power settings have been set, the camera gain should be optimized to provide the largest possible intensity dynamic range without saturating the detector.

7.3 Image Analysis

Materials

- Broad-emitting beads, Tetraspeck microspheres mounted on a slide (ThermoFisher Scientific T-14792)
- ImageJ with TrackMate plugin
- Matlab (Mathworks) software and scripts

Day 4 (Tracking)

1. Ensure that both channels are precisely registered. Cameras should be aligned prior to image acquisition using multicolor beads mounted on a standard slide. Any residual systematic offset between channels can be corrected using the translate function within ImageJ.
2. Particle tracking can be performed on a small number of frames (typically 3–5) to prevent biasing the analysis toward immobile particles.
3. Define a region of interest for analysis (eg, a single cell, nucleus, or cytoplasm).
4. Filter out randomly distributed noise using the FFT bandpass filter within ImageJ. Filter small objects below 3 pixels to reduce noise.

5. Detect spots using the Laplacian of Gaussian (LoG) detector in TrackMate (ImageJ). Spot size and thresholds should be optimized for detection of single mRNA particles.
6. Detected spots can be joined into trajectories in TrackMate using the linear assignment problem (LAP) tracker. The parameters linking max distance, gap-closing distance, and gap-closing max frame gap should be optimized as necessary to increase or reduce tracking stringency.
7. Use the visual inspector to ensure that particles are appropriately tracked.
8. Export tracking data as a spreadsheet.

Day 4 (Colocalization)

9. Colocalization analysis of trajectories is performed in Matlab (Mathworks) with custom written scripts.
10. Two tracks are considered to be colocalized if at least two spots of the green trajectory are within a pixel in x,y of a red trajectory.
11. Colocalization is then evaluated for accuracy by assessing individual colocalized trajectories.
12. Orphan red channel trajectories are identified as the translated mRNA fraction while the colocalized trajectories represent the mRNA fraction that has remained untranslated.

8. TRICK EXPERIMENT IN *DROSOPHILA*

Maternally deposited mRNAs of *D. melanogaster* encoding embryonic axis determinants such as *oskar*, *bicoid*, *gurken*, and *nanos* are frequently used as model systems to study mRNA transport and translational regulation. In the past, transport of these mRNAs has been successfully studied using transgenic animals expressing MS2-tagged reporter mRNAs (Forrest & Gavis, 2003; Jaramillo, Weil, Goodhouse, Gavis, & Schupbach, 2008; Weil, Forrest, & Gavis, 2006; Zimyanin et al., 2008). However, the insertion of MS2-binding sites has to be planned carefully in order to not destroy important *cis*-regulatory elements that are often located in the 3′-UTR and essential for proper transport and translational control (eg, oocyte entry signal (Jambor, Mueller, Bullock, & Ephrussi, 2014); translational control element (Gavis, Lunsford, Bergsten, & Lehmann, 1996)). Notably, some mRNAs such as *oskar* require splicing for transport and translational control (Ghosh, Marchand, Gaspar, & Ephrussi, 2012; Hachet & Ephrussi, 2004). We therefore always modify genomic DNA fragments.

To show the feasibility of imaging the first round of translation in *Drosophila*, we chose the *oskar* mRNA, which is produced in the nurse cells and transported over a long distance in order to localize to the posterior pole of

the developing oocyte, where it is finally translated. We used a genomic rescuing construct of 6.45 kb (Ephrussi & Lehmann, 1992) in which 6×MS2 loops were inserted into the 3′-UTR (Fig. 3A). This insertion has been previously used to study transport and has been shown to give rise to functional Oskar protein (Lin et al., 2008). Using the endogenous *oskar* promoter ensures that expression of the TRICK reporter is comparable to wild-type levels. In order to generate the functional *osk-TRICK* reporter, we inserted 12×PP7-binding sites in frame into the coding region (Fig. 3A). To generate transgenic animals, the full genomic region was subjected to P element-mediated germline transformation.

In order to provide the coat proteins necessary for labeling of the TRICK mRNA in the nurse cell nuclei, we express NLS-MCP-RFP and NLS-PCP-GFP fusion proteins under the control of a weak maternally active promoter, such as the *hsp83* promoter (Forrest & Gavis, 2003). Importantly, only this moderate expression of the coat proteins ensures no labeling artifacts, as seen by UAS-Gal4 driven constructs that produce nonspecific motile particles even in the absence of MS2-labeled mRNA (Xu, Brechbiel, & Gavis, 2013).

8.1 Imaging and Analysis

Materials

- 1 × PBS
- 16% paraformaldehyde solution (Electron Microscopy Sciences, #15710)
- Tween20 (Sigma, T9284)
- Triton X-100 (Sigma, P1379)
- BSA (bovine serum albumin, Sigma, A2153)
- Glass slides and coverslips
- Mounting solution (eg, Shandon Immu-Mount, Fisher Scientific, 9990402)

Protocol for *Drosophila* Oocytes

1. Dissect ovaries from well-fed female flies expressing *TRICK* mRNA, NLS-MCP-RFP, and NLS-PCP-GFP in 1 × PBS.
2. Replace PBS with fixative (1 × PBS supplemented with 4% paraformaldehyde) and incubate for 20 min.
3. Wash twice with PBST (1 × PBS, 0.1% Tween20).
4. Permeabilize ovaries for 1 h in 1 × PBS with 1% Triton X-100.
5. Wash twice with PBST (1 × PBS, 0.1% Tween20).
6. Block with blocking buffer (1 × PBST with 0.5% BSA) for 30 min.
7. Remove blocking buffer and add primary antibody (eg, anti-Oskar) in blocking buffer for 2 h.

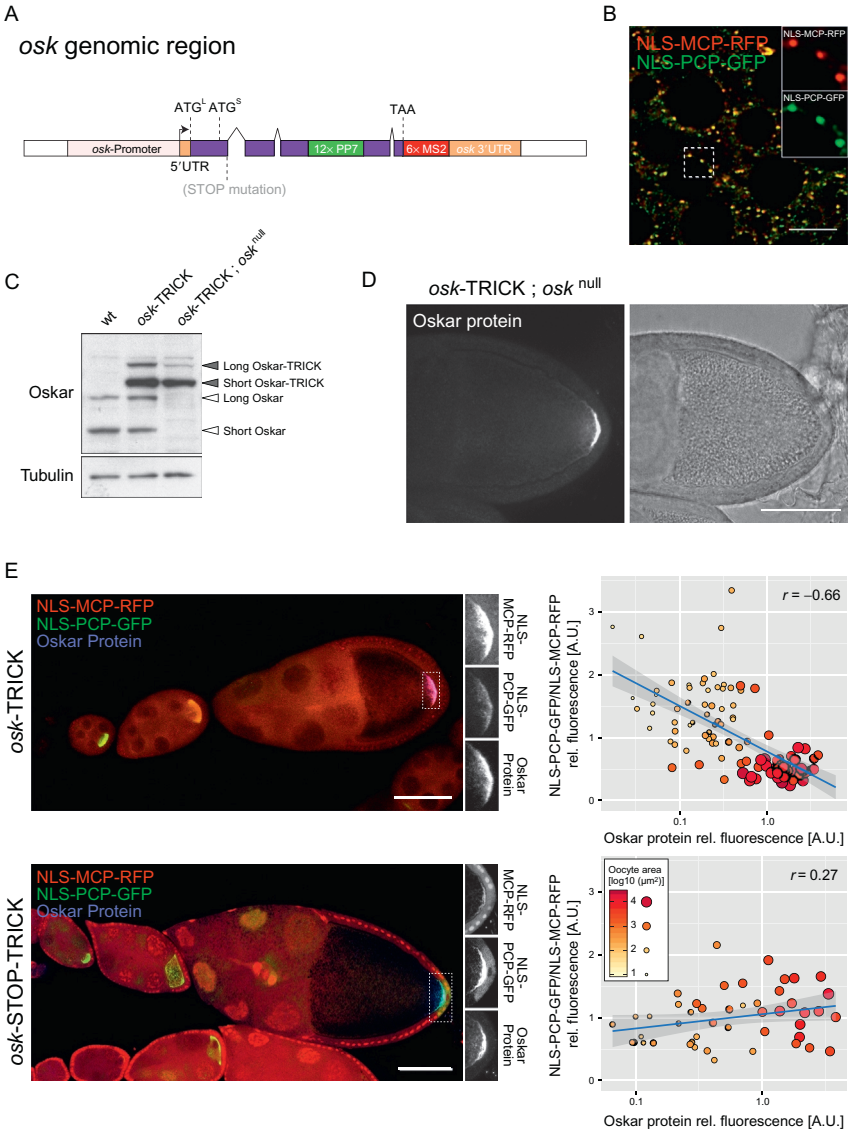

Fig. 3 TRICK in *Drosophila* oocytes. (A) Schematic of a genomic *osk*-TRICK reporter construct. The alternative translational start sites producing the long and short Oskar isoforms (ATG^L and ATG^S), the insertion site of 12×PP7 in the coding region, 6×MS2-binding sites right after the stop codon (TAA), and the position of the stop codon mutation used for control experiments are indicated. (B) Imaging of individual mRNPs in the ooplasm of an egg-chamber expressing *osk*-TRICK mRNA, NLS-MCP-RFP and NLS-PCP-GFP using FP-booster, scale bar 5 µm. (C) Insertion of 12xPP7-binding sites does not disturb translation of *oskar* mRNA. Western blot analysis of ovarian samples

8. Wash three times with PBST.
9. Incubate ovaries with secondary antibody conjugated to fluorophores spectrally distinct from EGFP and TagRFP-T (eg, Cy5, Alexa 647) in blocking buffer for 1 h.
10. Wash three times with PBST.
11. Separate individual egg-chambers, mount them on a glass slide using mounting solution and cover with a coverslip.
12. Acquire images on a standard wide-field or confocal microscope.
13. Images are further processed and the fluorescent signals and oocyte size of individual egg-chambers are measured using ImageJ (http://rsb.info.nih.gov/ij/). The ratio of NLS-PCP-GFP per NLS-MCP-RFP is calculated and plotted against the protein signal intensity and oocyte size.

Optional: *Drosophila* egg-chambers are relatively thick (from ~50 to >100 μm), which can present challenges for imaging. In order to obtain a good SNR, immunostaining with direct-coupled antibodies (eg, Anti-GFP-CF488A (Sigma, SAB4600051), RFP-booster (ChromoTek, rba594-100)) against FPs of the coat proteins can help to overcome this issue in fixed egg-chambers. This allows higher resolution imaging of individual RNA–protein particles containing *osk*-TRICK mRNA by confocal microscopy followed by deconvolution (Fig. 3B). Single-particle analysis can be carried out as described earlier.

8.2 Controls

As a first test for any defects in translation of the TRICK reporter transgenes, we recommend to use western blot analysis to identify the fusion protein derived from the *osk*-TRICK reporter, which appears with an increase in molecular weight of approximately 30 kDa caused by the extra polypeptide sequence derived from the 12×PP7-binding sites insertion (see Fig. 3C, middle lane). The use of mutant alleles to deplete any wild-type protein

from wild-type flies, flies expressing *osk*-TRICK and *osk*-TRICK in an osk^{null} background. (D) Immunostaining against Oskar protein in an egg-chamber expressing *osk*-TRICK in an osk^{null} background shows exclusive synthesis of Oskar protein at the posterior pole of the oocyte. (E) Quantification of fluorescent signals from NLS-PCP-GFP/NLS-MCP-RFP, Oskar protein immunostaining and oocyte area (color- and size-coded) of individual oocytes. The correlation of the TRICK reporter readout with Oskar protein and oocyte area observed in *osk*-TRICK expressing egg-chambers (*upper* plot) is abolished by the introduction of the STOP mutation prior the PP7-binding sites (*lower* plot). Pearson correlation coefficient (*r*), scale bars 50 μm.

allows standard immuno-fluorescence techniques and the use of well-established antibodies to detect protein derived exclusively from the TRICK reporter (Fig. 3C, right lane). This is important when considering the use of constructs in which the coding region and the PP7 loops are separated by a self-cleaving 2A peptide, making reporter and wild-type protein difficult to distinguish by mass.

Only at the posterior pole of the oocyte is translational repression of *oskar* mRNA relieved and Oskar protein produced. This process requires a precise orchestration of the transport machinery and translational regulators. Therefore, correct localization of Oskar protein exclusively at the posterior pole is a significant indicator of undisturbed regulation of the localized translation of the TRICK reporter construct. The use of mutant alleles (eg, osk^{null}) and standard immuno-fluorescence allows detection of Oskar protein solely derived from the *oskar*-TRICK reporter mRNA and confirms the correct localization of the protein independent of wild-type transcript and protein (Fig. 3D). This demonstrates that the introduction of PP7- and MS2-binding sites has no impact on the transport, translational repression, and translational activation of *osk*-TRICK mRNA.

Oskar protein first appears during mid-oogenesis (Kim-Ha, Kerr, & Macdonald, 1995), allowing a precise readout of the TRICK reporter performance to report on the translational status of *osk*-TRICK mRNA of individual egg-chambers during different developmental stages. A comparison of oocyte area, fluorescent intensities of Oskar protein immunostaining, and the NLS-PCP-GFP to NLS-MCP-RFP ratio shows the correlation of loss of NLS-PCP-GFP signal with oocyte size and Oskar protein appearance (Fig. 3E). In order to demonstrate that the observed loss of the NLS-PCP-GFP signal in later stage oocytes depends on active translation, introduction of a STOP codon by site-directed mutagenesis upstream of the PP7-binding sites of the *osk-TRICK* mRNA (*osk*-STOP-TRICK) should be used (Fig. 3E). Similar to TRICK experiments in cultured mammalian cells, small-molecule inhibitors of translation can also be used.

TRICK reporter mRNAs can be used to monitor the first round of translation with single mRNP resolution in the animal model system *Drosophila*, a powerful resource with established genetic toolboxes and well-studied examples of localized translation.

9. OUTLOOK

The development of multiple orthogonal fluorescent labeling methodologies for imaging single molecules of RNA in living cells has made it

possible to perform more detailed analyses of RNA metabolism. RNA biosensors, which go beyond simply being able to observe mRNAs, enable direct measurement of specific events in an mRNA's life. We have engineered the TRICK system that reports on the first round of translation, but we envision that conceptually similar approaches may also be applied to mRNA turnover and other aspects of RNA metabolism. These advances coupled to the revolution in genome engineering tools will allow the complete lives of endogenous mRNAs to be imaged in living cells.

ACKNOWLEDGMENTS

This work was supported by the Novartis Research Foundation and the Swiss National Science Foundation (J.A.C); the European Molecular Biology Lab (A.E.); and postdoctoral fellowships from the Peter and Traudl Engelhorn Foundation (J.M.H) and the EMBL Interdisciplinary Postdoc Program (EIPOD) under Marie Curie COFUND actions (F.W.).

REFERENCES

Aitken, C. E., Marshall, R. A., & Puglisi, J. D. (2008). An oxygen scavenging system for improvement of dye stability in single-molecule fluorescence experiments. *Biophysical Journal*, *94*(5), 1826–1835.

Bertrand, E., Chartrand, P., Schaefer, M., Shenoy, S. M., Singer, R. H., & Long, R. M. (1998). Localization of ASH1 mRNA particles in living yeast. *Molecular Cell*, *2*(4), 437–445.

Chao, J. A., Patskovsky, Y., Almo, S. C., & Singer, R. H. (2008). Structural basis for the coevolution of a viral RNA-protein complex. *Nature Structural & Molecular Biology*, *15*(1), 103–105.

Chen, J., Nikolaitchik, O., Singh, J., Wright, A., Bencsics, C. E., Coffin, J. M., … Hu, W. S. (2009). High efficiency of HIV-1 genomic RNA packaging and heterozygote formation revealed by single virion analysis. *Proceedings of the National Academy of Sciences of the United States of America*, *106*(32), 13535–13540.

Chenouard, N., Smal, I., de Chaumont, F., Maska, M., Sbalzarini, I. F., Gong, Y., … Meijering, E. (2014). Objective comparison of particle tracking methods. *Nature Methods*, *11*(3), 281–289.

Cho, S., Jang, J., Song, C., Lee, H., Ganesan, P., Yoon, T. Y., … Park, Y. (2013). Simple super-resolution live-cell imaging based on diffusion-assisted Forster resonance energy transfer. *Scientific Reports*, *3*, 1208.

Coulon, A., Ferguson, M. L., de Turris, V., Palangat, M., Chow, C. C., & Larson, D. R. (2014). Kinetic competition during the transcription cycle results in stochastic RNA processing. *Elife*, *3*, e03939.

Daigle, N., & Ellenberg, J. (2007). LambdaN-GFP: An RNA reporter system for live-cell imaging. *Nature Methods*, *4*(8), 633–636.

David, A., Dolan, B. P., Hickman, H. D., Knowlton, J. J., Clavarino, G., Pierre, P., … Yewdell, J. W. (2012). Nuclear translation visualized by ribosome-bound nascent chain puromycylation. *The Journal of Cell Biology*, *197*(1), 45–57.

Deschout, H., Martens, T., Vercauteren, D., Remaut, K., Demeester, J., De Smedt, S. C., … Braeckmans, K. (2013). Correlation of dual colour single particle trajectories for improved detection and analysis of interactions in living cells. *International Journal of Molecular Sciences*, *14*(8), 16485–16514.

Dieterich, D. C., Hodas, J. J., Gouzer, G., Shadrin, I. Y., Ngo, J. T., Triller, A., … Schuman, E. M. (2010). In situ visualization and dynamics of newly synthesized proteins in rat hippocampal neurons. *Nature Neuroscience*, *13*(7), 897–905.

Dupont, A., Stirnnagel, K., Lindemann, D., & Lamb, D. C. (2013). Tracking image correlation: Combining single-particle tracking and image correlation. *Biophysical Journal*, *104*(11), 2373–2382.

Ephrussi, A., & Lehmann, R. (1992). Induction of germ cell formation by oskar. *Nature*, *358*(6385), 387–392.

Espenel, C., Margeat, E., Dosset, P., Arduise, C., Le Grimellec, C., Royer, C. A., … Milhiet, P. E. (2008). Single-molecule analysis of CD9 dynamics and partitioning reveals multiple modes of interaction in the tetraspanin web. *The Journal of Cell Biology*, *182*(4), 765–776.

Forrest, K. M., & Gavis, E. R. (2003). Live imaging of endogenous RNA reveals a diffusion and entrapment mechanism for nanos mRNA localization in *Drosophila*. *Current Biology*, *13*(14), 1159–1168.

Fusco, D., Accornero, N., Lavoie, B., Shenoy, S. M., Blanchard, J. M., Singer, R. H., & Bertrand, E. (2003). Single mRNA molecules demonstrate probabilistic movement in living mammalian cells. *Current Biology*, *13*(2), 161–167.

Gautier, A., Juillerat, A., Heinis, C., Correa, I. R., Kindermann, M., Beaufils, F., & Johnsson, K. (2008). An engineered protein tag for multiprotein labeling in living cells. *Chemistry & Biology*, *15*(2), 128–136.

Gavis, E. R., Lunsford, L., Bergsten, S. E., & Lehmann, R. (1996). A conserved 90 nucleotide element mediates translational repression of nanos RNA. *Development*, *122*(9), 2791–2800.

Gerhardt, I., Mai, L., Lamas-Linares, A., & Kurtsiefer, C. (2011). Detection of single molecules illuminated by a light-emitting diode. *Sensors (Basel)*, *11*(1), 905–916.

Ghosh, S., Marchand, V., Gaspar, I., & Ephrussi, A. (2012). Control of RNP motility and localization by a splicing-dependent structure in oskar mRNA. *Nature Structural & Molecular Biology*, *19*(4), 441–449.

Gossen, M., Freundlieb, S., Bender, G., Muller, G., Hillen, W., & Bujard, H. (1995). Transcriptional activation by tetracyclines in mammalian cells. *Science*, *268*(5218), 1766–1769.

Grimm, J. B., English, B. P., Chen, J., Slaughter, J. P., Zhang, Z., Revyakin, A., & Lavis, L. D. (2015). A general method to improve fluorophores for live-cell and single-molecule microscopy. *Nature Methods*, *12*(3), 244–250. 243 pp. following 250 pp.

Grunwald, D., & Singer, R. H. (2010). In vivo imaging of labelled endogenous beta-actin mRNA during nucleocytoplasmic transport. *Nature*, *467*(7315), 604–607.

Hachet, O., & Ephrussi, A. (2004). Splicing of oskar RNA in the nucleus is coupled to its cytoplasmic localization. *Nature*, *428*(6986), 959–963.

Halstead, J. M., Lionnet, T., Wilbertz, J. H., Wippich, F., Ephrussi, A., Singer, R. H., & Chao, J. A. (2015). Translation. An RNA biosensor for imaging the first round of translation from single cells to living animals. *Science*, *347*(6228), 1367–1671.

Higashida, C., Suetsugu, S., Tsuji, T., Monypenny, J., Narumiya, S., & Watanabe, N. (2008). G-actin regulates rapid induction of actin nucleation by mDia1 to restore cellular actin polymers. *Journal of Cell Science*, *121*(Pt. 20), 3403–3412.

Hocine, S., Raymond, P., Zenklusen, D., Chao, J. A., & Singer, R. H. (2013). Single-molecule analysis of gene expression using two-color RNA labeling in live yeast. *Nature Methods*, *10*(2), 119–121.

Holt, C. E., & Schuman, E. M. (2013). The central dogma decentralized: New perspectives on RNA function and local translation in neurons. *Neuron*, *80*(3), 648–657.

Ifrim, M. F., Williams, K. R., & Bassell, G. J. (2015). Single-molecule imaging of PSD-95 mRNA translation in dendrites and its dysregulation in a mouse model of fragile

X syndrome. *The Journal of Neuroscience*, *35*(18), 7116–7130. http://dx.doi.org/10.1523/JNEUROSCI.2802-14.2015.

Ingolia, N. T., Ghaemmaghami, S., Newman, J. R., & Weissman, J. S. (2009). Genome-wide analysis in vivo of translation with nucleotide resolution using ribosome profiling. *Science*, *324*(5924), 218–223.

Ishigaki, Y., Li, X., Serin, G., & Maquat, L. E. (2001). Evidence for a pioneer round of mRNA translation: mRNAs subject to nonsense-mediated decay in mammalian cells are bound by CBP80 and CBP20. *Cell*, *106*(5), 607–617.

Jambor, H., Mueller, S., Bullock, S. L., & Ephrussi, A. (2014). A stem-loop structure directs oskar mRNA to microtubule minus ends. *RNA*, *20*(4), 429–439.

Jan, C. H., Williams, C. C., & Weissman, J. S. (2014). Principles of ER cotranslational translocation revealed by proximity-specific ribosome profiling. *Science*, *346*(6210), 1257521.

Jaramillo, A. M., Weil, T. T., Goodhouse, J., Gavis, E. R., & Schupbach, T. (2008). The dynamics of fluorescently labeled endogenous gurken mRNA in *Drosophila*. *Journal of Cell Science*, *121*(Pt. 6), 887–894.

Juillerat, A., Gronemeyer, T., Keppler, A., Gendreizig, S., Pick, H., Vogel, H., & Johnsson, K. (2003). Directed evolution of O-6-alkylguanine-DNA alkyltransferase for efficient labeling of fusion proteins with small molecules in vivo. *Chemistry & Biology*, *10*(4), 313–317.

Kim, J. H., Lee, S. R., Li, L. H., Park, H. J., Park, J. H., Lee, K. Y., … Choi, S. Y. (2011). High cleavage efficiency of a 2A peptide derived from porcine teschovirus-1 in human cell lines, zebrafish and mice. *PloS One*, *6*(4), e18556.

Kim-Ha, J., Kerr, K., & Macdonald, P. M. (1995). Translational regulation of oskar mRNA by bruno, an ovarian RNA-binding protein, is essential. *Cell*, *81*(3), 403–412.

Koyama-Honda, I., Ritchie, K., Fujiwara, T., Iino, R., Murakoshi, H., Kasai, R. S., & Kusumi, A. (2005). Fluorescence imaging for monitoring the colocalization of two single molecules in living cells. *Biophysical Journal*, *88*(3), 2126–2136.

Kremers, G. J., Gilbert, S. G., Cranfill, P. J., Davidson, M. W., & Piston, D. W. (2011). Fluorescent proteins at a glance. *Journal of Cell Science*, *124*(Pt. 2), 157–160.

Kumano, G. (2012). Polarizing animal cells via mRNA localization in oogenesis and early development. *Development, Growth & Differentiation*, *54*(1), 1–18.

Kuo, J. S., Kuyper, C. L., Allen, P. B., Fiorini, G. S., & Chiu, D. T. (2004). High-power blue/UV light-emitting diodes as excitation sources for sensitive detection. *Electrophoresis*, *25*(21–22), 3796–3804.

Larson, D. R., Zenklusen, D., Wu, B., Chao, J. A., & Singer, R. H. (2011). Real-time observation of transcription initiation and elongation on an endogenous yeast gene. *Science*, *332*(6028), 475–478.

Liao, G., Mingle, L., Van De Water, L., & Liu, G. (2015). Control of cell migration through mRNA localization and local translation. *Wiley Interdisciplinary Reviews. RNA*, *6*(1), 1–15.

Lin, M. D., Jiao, X., Grima, D., Newbury, S. F., Kiledjian, M., & Chou, T. B. (2008). *Drosophila* processing bodies in oogenesis. *Developmental Biology*, *322*(2), 276–288.

Lionnet, T., Czaplinski, K., Darzacq, X., Shav-Tal, Y., Wells, A. L., Chao, J. A., … Singer, R. H. (2011). A transgenic mouse for in vivo detection of endogenous labeled mRNA. *Nature Methods*, *8*(2), 165–170.

Los, G. V., Encell, L. P., McDougall, M. G., Hartzell, D. D., Karassina, N., Zimprich, C., … Wood, K. V. (2008). HatoTag: A novel protein labeling technology for cell imaging and protein analysis. *ACS Chemical Biology*, *3*(6), 373–382.

Ma, J., Liu, Z., Michelotti, N., Pitchiaya, S., Veerapaneni, R., Androsavich, J. R., … Yang, W. (2013). High-resolution three-dimensional mapping of mRNA export through the nuclear pore. *Nature Communications*, *4*, 2414.

Magidson, V., & Khodjakov, A. (2013). Circumventing photodamage in live-cell microscopy. *Methods in Cell Biology*, *114*, 545–560.
Martin, R. M., Rino, J., Carvalho, C., Kirchhausen, T., & Carmo-Fonseca, M. (2013). Live-cell visualization of pre-mRNA splicing with single-molecule sensitivity. *Cell Reports*, *4*(6), 1144–1155.
Mizuguchi, H., Xu, Z., Ishii-Watabe, A., Uchida, E., & Hayakawa, T. (2000). IRES-dependent second gene expression is significantly lower than cap-dependent first gene expression in a bicistronic vector. *Molecular Therapy*, *1*(4), 376–382.
Mor, A., Suliman, S., Ben-Yishay, R., Yunger, S., Brody, Y., & Shav-Tal, Y. (2010). Dynamics of single mRNP nucleocytoplasmic transport and export through the nuclear pore in living cells. *Nature Cell Biology*, *12*(6), 543–552.
No, D., Yao, T. P., & Evans, R. M. (1996). Ecdysone-inducible gene expression in mammalian cells and transgenic mice. *Proceedings of the National Academy of Sciences of the United States of America*, *93*(8), 3346–3351.
Pan, D., Kirillov, S. V., & Cooperman, B. S. (2007). Kinetically competent intermediates in the translocation step of protein synthesis. *Molecular Cell*, *25*(4), 519–529.
Park, H. Y., Buxbaum, A. R., & Singer, R. H. (2010). Single mRNA tracking in live cells. *Methods in Enzymology*, *472*, 387–406.
Park, H. Y., Lim, H., Yoon, Y. J., Follenzi, A., Nwokafor, C., Lopez-Jones, M., … Singer, R. H. (2014). Visualization of dynamics of single endogenous mRNA labeled in live mouse. *Science*, *343*(6169), 422–424.
Parthasarathy, R. (2012). Rapid, accurate particle tracking by calculation of radial symmetry centers. *Nature Methods*, *9*(7), 724–726.
Qin, J. Y., Zhang, L., Clift, K. L., Hulur, I., Xiang, A. P., Ren, B. Z., & Lahn, B. T. (2010). Systematic comparison of constitutive promoters and the doxycycline-inducible promoter. *PLoS One*, *5*(5), e10611.
Rabut, G., & Ellenberg, J. (2004). Automatic real-time three-dimensional cell tracking by fluorescence microscopy. *Journal of Microscopy*, *216*(Pt. 2), 131–137.
Rasnik, I., McKinney, S. A., & Ha, T. (2006). Nonblinking and long-lasting single-molecule fluorescence imaging. *Nature Methods*, *3*(11), 891–893.
Shaner, N. C., Lin, M. Z., McKeown, M. R., Steinbach, P. A., Hazelwood, K. L., Davidson, M. W., & Tsien, R. Y. (2008). Improving the photostability of bright monomeric orange and red fluorescent proteins. *Nature Methods*, *5*(6), 545–551.
Shaner, N. C., Steinbach, P. A., & Tsien, R. Y. (2005). A guide to choosing fluorescent proteins. *Nature Methods*, *2*(12), 905–909.
Shav-Tal, Y., Darzacq, X., Shenoy, S. M., Fusco, D., Janicki, S. M., Spector, D. L., & Singer, R. H. (2004). Dynamics of single mRNPs in nuclei of living cells. *Science*, *304*(5678), 1797–1800.
Smith, C. S., Preibisch, S., Joseph, A., Abrahamsson, S., Rieger, B., Myers, E., … Grunwald, D. (2015). Nuclear accessibility of beta-actin mRNA is measured by 3D single-molecule real-time tracking. *The Journal of Cell Biology*, *209*(4), 609–619.
Spille, J. H., Kaminski, T. P., Scherer, K., Rinne, J. S., Heckel, A., & Kubitscheck, U. (2015). Direct observation of mobility state transitions in RNA trajectories by sensitive single molecule feedback tracking. *Nucleic Acids Research*, *43*(2), e14.
Steitz, J. A. (1969). Nucleotide sequences of the ribosomal binding sites of bacteriophage R17 RNA. *Cold Spring Harbor Symposia on Quantitative Biology*, *34*, 621–630.
Takizawa, P. A., & Vale, R. D. (2000). The myosin motor, Myo4p, binds Ash1 mRNA via the adapter protein, She3p. *Proceedings of the National Academy of Sciences of the United States of America*, *97*(10), 5273–5278.
Tatavarty, V., Ifrim, M. F., Levin, M., Korza, G., Barbarese, E., Yu, J., & Carson, J. H. (2012). Single-molecule imaging of translational output from individual RNA granules in neurons. *Molecular Biology of the Cell*, *23*(5), 918–929.

Terskikh, A., Fradkov, A., Ermakova, G., Zaraisky, A., Tan, P., Kajava, A. V., … Siebert, P. (2000). "Fluorescent timer": Protein that changes color with time. *Science*, *290*(5496), 1585–1588.

Thompson, R. E., Larson, D. R., & Webb, W. W. (2002). Precise nanometer localization analysis for individual fluorescent probes. *Biophysical Journal*, *82*(5), 2775–2783.

Tokunaga, M., Imamoto, N., & Sakata-Sogawa, K. (2008). Highly inclined thin illumination enables clear single-molecule imaging in cells. *Nature Methods*, *5*(2), 159–161.

Urbanek, M. O., Galka-Marciniak, P., Olejniczak, M., & Krzyzosiak, W. J. (2014). RNA imaging in living cells—Methods and applications. *RNA Biology*, *11*(8), 1083–1095.

Vigers, G. P., Coue, M., & McIntosh, J. R. (1988). Fluorescent microtubules break up under illumination. *The Journal of Cell Biology*, *107*(3), 1011–1024.

Weidenfeld, I., Gossen, M., Low, R., Kentner, D., Berger, S., Gorlich, D., … Schonig, K. (2009). Inducible expression of coding and inhibitory RNAs from retargetable genomic loci. *Nucleic Acids Research*, *37*(7), e50.

Weil, T. T., Forrest, K. M., & Gavis, E. R. (2006). Localization of bicoid mRNA in late oocytes is maintained by continual active transport. *Developmental Cell*, *11*(2), 251–262.

Widengren, J., Chmyrov, A., Eggeling, C., Lofdahl, P. A., & Seidel, C. A. (2007). Strategies to improve photostabilities in ultrasensitive fluorescence spectroscopy. *The Journal of Physical Chemistry. A*, *111*(3), 429–440.

Wu, B., Chao, J. A., & Singer, R. H. (2012). Fluorescence fluctuation spectroscopy enables quantitative imaging of single mRNAs in living cells. *Biophysical Journal*, *102*(12), 2936–2944.

Wu, B., Miskolci, V., Sato, H., Tutucci, E., Kenworthy, C. A., Donnelly, S. K., … Hodgson, L. (2015). Synonymous modification results in high-fidelity gene expression of repetitive protein and nucleotide sequences. *Genes & Development*, *29*(8), 876–886.

Xia, T., Li, N., & Fang, X. (2013). Single-molecule fluorescence imaging in living cells. *Annual Review of Physical Chemistry*, *64*, 459–480.

Xu, X., Brechbiel, J. L., & Gavis, E. R. (2013). Dynein-dependent transport of nanos RNA in *Drosophila* sensory neurons requires Rumpelstiltskin and the germ plasm organizer Oskar. *The Journal of Neuroscience*, *33*(37), 14791–14800.

Yu, J., Xiao, J., Ren, X., Lao, K., & Xie, X. S. (2006). Probing gene expression in live cells, one protein molecule at a time. *Science*, *311*(5767), 1600–1603.

Zimyanin, V. L., Belaya, K., Pecreaux, J., Gilchrist, M. J., Clark, A., Davis, I., & St Johnston, D. (2008). In vivo imaging of oskar mRNA transport reveals the mechanism of posterior localization. *Cell*, *134*(5), 843–853.

Zuker, M. (2003). Mfold web server for nucleic acid folding and hybridization prediction. *Nucleic Acids Research*, *31*(13), 3406–3415.